



Title	Cherenkov counting of $^{90}\text{Sr}$ and $^{90}\text{Y}$ in bark and leaf samples collected around Fukushima Daiichi Nuclear Power Plant
Author(s)	Kubota, Takumi; Shibahara, Yuji; Fukutani, Satoshi; Fujii, Toshiyuki; Ohta, Tomoko; Kowatari, Munehiko; Mizuno, Satoshi; Takamiya, Koichi; Yamana, Hajimu
Citation	Journal of Radioanalytical and Nuclear Chemistry, 303(1), 39-46 <a href="https://doi.org/10.1007/s10967-014-3348-y">https://doi.org/10.1007/s10967-014-3348-y</a>
Issue Date	2015-01
Doc URL	<a href="http://hdl.handle.net/2115/57992">http://hdl.handle.net/2115/57992</a>
Type	article (author version)
File Information	JRNC2015.303.39-46.pdf



[Instructions for use](#)

1 **Cherenkov counting of <sup>90</sup>Sr and <sup>90</sup>Y in bark and leaf samples collected around Fukushima Daiichi**  
2 **Nuclear Power Plant**

3  
4 Takumi KUBOTA<sup>1)\*</sup>, Yuji SHIBAHARA<sup>1)</sup>, Satoshi FUKUTANI<sup>1)</sup>, Toshiyuki FUJII<sup>1)</sup>, Tomoko OHTA<sup>2)</sup>,  
5 Munehiko KOWATARI<sup>3)</sup>, Satoshi MIZUNO<sup>4)</sup>, Kohichi TAKAMIYA<sup>1)</sup>, Hajimu YAMANA<sup>1)</sup>

6  
7 1) Research Reactor Institute, Kyoto University, Kumatori, Osaka 590-0494, Japan

8 2) Hokkaido University, Sapporo, Hokkaido 060-8628, Japan

9 3) Japan Atomic Energy Agency, Tokai, Ibaragi 319-1195, Japan

10 4) Nuclear Power Safety Division, Fukushima Prefectural Government, Fukushima 960-8043, Japan

11 \*Corresponding author: t\_kubota@rri.kyoto-u.ac.jp

12  
13 **Abstract**

14 The radioactivity of <sup>90</sup>Sr and <sup>137</sup>Cs in environmental samples, bark and leaf, collected around the  
15 Fukushima Daiichi Nuclear Power Plant in May 2013 was determined with the aim of investigating the  
16 migration of both nuclides using their radioactivity ratio. The radioactivity of <sup>90</sup>Sr was determined by  
17 using Cherenkov counting of <sup>90</sup>Y after purification using Sr resin and that of <sup>137</sup>Cs was determined by  
18  $\gamma$ -spectrometry. Quench correction in Cherenkov counting was investigated by measurements of samples  
19 spiked with purified <sup>90</sup>Y revealed that the radioactivity could be evaluated without quench correction. The  
20 radioactivity ratio of <sup>90</sup>Sr to <sup>137</sup>Cs in bark samples of  $4.2 \times 10^{-3}$  and  $1.2 \times 10^{-2}$  was compared with the results  
21 from soil samples collected in July 2011 to show that the migration of <sup>90</sup>Sr was slower than <sup>137</sup>Cs in bark  
22 and tree.

23  
24 **Keywords:** strontium-90, cesium-137, Cherenkov counting, Fukushima nuclear accident, vegetation  
25 samples

26  
27 **Introduction**

28 The accident at the Fukushima Daiichi Nuclear Power Plant led to the release of a large amount of  
29 various radioactive materials, which migrated through the atmosphere, hydrosphere, and biosphere and a  
30 part of which were chemically and physically trapped in the environment. Among the radioactive nuclides  
31 released as a result of the Fukushima accident, the environmental contamination from radioiodine and  
32 radiocesium has been well-studied previously [1-6]; these studies have reported that radioiodine spread  
33 globally while radiocesium was mainly deposited in East Japan and released into the Pacific Ocean.  
34 Radioactive strontium, not well-studied in the wake of the Fukushima accident, is still important to  
35 investigate for its migration into vegetation and accumulation in foodstuff in terms of internal exposure.

36 <sup>89</sup>Sr and <sup>90</sup>Sr, unlike <sup>137</sup>Cs and <sup>131</sup>I, are pure beta emitter nuclides, and their radioactive  
37 measurements should be conducted after the purification of strontium from the sample matrix. Methods  
38 for purification include the use of a specific resin [7-11], solvent extraction [12], and anion exchange  
39 resin [13,14]. Radioactivity levels are then often determined using a gas flow proportional counter  
40 [7,8,11,15,16] and a liquid scintillation counter that employs scintillation fluid [10,17-21] or Cherenkov

41 radiation [13,14,22]. Methods that utilize Cherenkov radiation are generally more practical because the  
42 sample solution can be measured without mixing extra fluids, which prevents the recovery of the  
43 strontium fraction.

44 We determined the radioactivity of  $^{90}\text{Sr}$  and  $^{137}\text{Cs}$  in vegetation samples collected in the vicinity of  
45 the Fukushima Daiichi Nuclear Power Plant, where agricultural activities are prohibited due to high-level  
46 radioactive contamination. Thus, we collected bark and leaf samples instead of agricultural samples and  
47 investigated the migration of both nuclides in bark and tree in comparison to the radioactivity of soil  
48 samples [23]. In order to validate the Cherenkov counting for the determination of  $^{90}\text{Sr}$ , we evaluated the  
49 extent of the quench effect by measuring and comparing the samples with and without the spike of  $^{90}\text{Y}$   
50 solution.

51

## 52 **Materials and Methods**

53 We collected vegetation samples around the Fukushima Daiichi Nuclear Power Plant from 25–28  
54 May 2013. Bark and fresh leaves from *Cryptomeria japonica* and fresh leaves from *Artemisia indica* var.  
55 *maximowiczii* were collected from plants 3 km north of the power plant's Unit No. 1, and bark from  
56 *Metasequoia glyptostroboides* was collected from plants 2 km south of the unit. Air dose rates at 1 m  
57 height were measured at 1  $\mu\text{Sv/h}$  and 30  $\mu\text{Sv/h}$  from the north and south locations, respectively.

58 The vegetation samples were washed with distilled water under an ultrasonic wave to remove soil  
59 particles from the surface of the vegetation samples. The wet samples and the resulting suspended  
60 solution were dried at approximately 100 °C, packed in plastic bags and bottles, and stored in a desiccator  
61 before further treatment. An aliquot of each vegetation sample (2.5 g dry weight) was placed in a quartz  
62 test tube and incinerated at 600 °C in a tubular furnace. The ashed samples were then dissolved in hot  
63 concentrated nitric acid, fumed to dryness, dissolved in 0.1 M  $\text{HNO}_3$ , and centrifuged into separate  
64 supernatants. The resulting solution for each sample was treated with cation exchange resin Dowex  
65 50WX8 (100–200 mesh), Eichrom UTEVA-resin (100–150  $\mu\text{m}$ ), and Eichrom Sr resin (100–150  $\mu\text{m}$ ) to  
66 purify the strontium fraction [24]. The strontium fraction, contained in the supernatant solution in 50 mL  
67 of 0.1 M  $\text{HNO}_3$ , was loaded into 4 mL of cation exchange resin and recovered with 20 mL of 8 M  $\text{HNO}_3$   
68 following a resin wash with 0.1 M  $\text{HNO}_3$ . The recovered strontium was then injected into a column filled  
69 with 1 mL of UTEVA resin to remove uranium and plutonium. The strontium fraction eluted into the first  
70 effluent was fumed to dryness and prepared to 10 mL of 3 M  $\text{HNO}_3$  solution. This solution was injected  
71 into a column filled with 1 mL of Sr resin, resin washed with 5 mL of 3 M  $\text{HNO}_3$ , and treated with 20 mL  
72 of 0.05 M  $\text{HNO}_3$  to recover the strontium fraction. Finally, for each sample, the radioactivity levels of  $^{90}\text{Sr}$   
73 and  $^{90}\text{Y}$  in the purified strontium solution were measured by Cherenkov counting and the recovery of  
74 strontium throughout the purification was evaluated using an inductively coupled plasma quadrupole  
75 mass spectrometry (ICP-QMS, HP-4500, Yokogawa).

76 The Cherenkov radiation from an aliquot of the purified strontium solution (10 mL) was measured  
77 with a liquid scintillation analyzer (Tri-Carb 2700 TR, Packard), with Milli-Q water used to obtain the  
78 background value. The radioactivity of  $^{137}\text{Cs}$ , which accounted for dominant levels of radioactivity in the  
79 samples collected around the Fukushima Daiichi Nuclear Power Plant, was measured by  $\gamma$ -spectrometry  
80 (a coaxial-type Ge detector, Canberra). For this measurement, energy calibration was conducted with a

81 certified calibration standard source ( $^{109}\text{Cd}$ ,  $^{57}\text{Co}$ ,  $^{139}\text{Ce}$ ,  $^{203}\text{Hg}$ ,  $^{113}\text{Sn}$ ,  $^{85}\text{Sr}$ ,  $^{137}\text{Cs}$ ,  $^{88}\text{Y}$ , and  $^{60}\text{Co}$ ; GE  
 82 Healthcare), and solid angle correction factors were determined with potassium chloride powder and  
 83 solution [25,26].

84 The calibration of the Cherenkov counting, the evaluation of its coefficient, and the correction of  
 85 quenching in the counting were conducted using  $^{134}\text{Cs}$  generated at the Kyoto University Research  
 86 Reactor (KUR) [27] and the standard solution of  $^{90}\text{Sr}$  was purchased from Eckert and Ziegler Isotope  
 87 Products. The counting coefficients of  $^{90}\text{Sr}$  and  $^{90}\text{Y}$  were obtained from the increase in the radioactivity of  
 88  $^{90}\text{Y}$  in the purified  $^{90}\text{Sr}$  solution. The calculation is described below. The correction of quenching was  
 89 conducted by the spiking of purified  $^{90}\text{Y}$  solution to the sample strontium solution and nitric acid, as  
 90 control for quenching, for comparison after quantitative analysis. The difference of the resulting increase  
 91 in counting rate between both solutions showed a need to correct for quenching. Purified  $^{90}\text{Y}$ , absent of  
 92  $^{90}\text{Sr}$ , was spiked to avoid the spoil of sample strontium solution, whose radioactivity was finally regulated  
 93 by the original  $^{90}\text{Sr}$  after the decay of the extra radioactivity of  $^{90}\text{Y}$ . The separation of  $^{90}\text{Sr}$  and  $^{90}\text{Y}$  from  
 94 the standard solution was conducted by using the Sr resin method, as described above, and the radioactive  
 95 purity of both fractions were 99.9%.

96

### 97 Calculations

98 We quantified levels of  $^{90}\text{Sr}$  using the radioactivity of its daughter nuclide,  $^{90}\text{Y}$ , which required long  
 99 periods of time for measuring low-level samples. The change in  $^{90}\text{Y}$  radioactivity during measurements  
 100 must be accounted for in this process because of its relatively short half-life, and corrections for decay  
 101 and growth are described in detail below. The radioactivity levels of environmental samples due to  $^{90}\text{Sr}$   
 102 were calculated using regression analysis, with the  $^{90}\text{Y}$  and  $^{90}\text{Sr}$  measurement coefficient.

103 When radioactivity changes during measurements, the counting rate  $C$  (e.g., count per minute  
 104 (CPM)) can be expressed according to the following equation:

$$105 \quad C = \frac{1}{t_d} \int_{t_l}^{t_l+t_d} \sum \varepsilon_i A_i(t) dt + BG \quad (1)$$

106 where  $t_d$  is counting time,  $t_l$  is the start time of counting,  $\varepsilon_i$  and  $A_i$  are the measurement coefficient and  
 107 the radioactivity, respectively, of nuclide  $i$  (i.e.,  $i = ^{90}\text{Y}$ ,  $^{90}\text{Sr}$ ,  $^{134}\text{Cs}$ ,  $^{137}\text{Cs}$ ,  $^{40}\text{K}$ , etc.) with the radioactivity  
 108 of  $^{89}\text{Sr}$  ignored because of its short half life causes it to decay away before the sample collection, and  $BG$   
 109 is the background value derived from the blank measurement. We used this equation for the correction of  
 110 growth for  $^{90}\text{Y}$ . The net counting rate (net CPM),  $Y$ , was then expressed according to the following  
 111 equation:

$$112 \quad Y = C - BG \quad (2)$$

113 Both measurement coefficients for  $^{90}\text{Y}$  and  $^{90}\text{Sr}$  were evaluated from the measurement of a standard  
 114  $^{90}\text{Sr}$  solution in equilibrium, completely eliminated of  $^{90}\text{Y}$ . For the measurement of the  $^{90}\text{Sr}$  solution with  
 115 the growth of  $^{90}\text{Y}$ , Eq. (1) can be modified to the following equation:

$$116 \quad Y = \frac{1}{t_d} \int_{t_l}^{t_l+t_d} \varepsilon_{\text{Y-90}} A_{\text{Y-90}}(t) dt + \varepsilon_{\text{Sr-90}} A_{\text{Sr-90}}^0 \quad (3)$$

117 where  $A_{\text{Sr-90}}^0$  is the initial radioactivity of  $^{90}\text{Sr}$  and its decay is ignored for the short period. The

118 radioactivity of  $^{90}\text{Y}$ ,  $A_{\text{Y-90}}(t)$ , produced through the decay of  $^{90}\text{Sr}$ , can be expressed according to the  
 119 following equation:

$$120 \quad A_{\text{Y-90}}(t) = \frac{\lambda_{\text{Y-90}}}{\lambda_{\text{Y-90}} - \lambda_{\text{Sr-90}}} A_{\text{Sr-90}}^0 \left( e^{-\lambda_{\text{Sr-90}}t} - e^{-\lambda_{\text{Y-90}}t} \right) \quad (4)$$

121 where  $\lambda_{\text{Y-90}}$  and  $\lambda_{\text{Sr-90}}$  are the decay constants of  $^{90}\text{Y}$  and  $^{90}\text{Sr}$ , respectively, and the initial  
 122 radioactivity of  $^{90}\text{Y}$  is zero as  $^{90}\text{Y}$  is eliminated by the separation of  $^{90}\text{Sr}$ . In the short period where the  
 123 decay of  $^{90}\text{Sr}$  can be ignored, the relationship between both decay constants,  $\lambda_{\text{Y-90}} \gg \lambda_{\text{Sr-90}}$ ,  
 124 simplifies the equation to the following:

$$125 \quad A_{\text{Y-90}}(t) = A_{\text{Sr-90}}^0 \left( 1 - e^{-\lambda_{\text{Y-90}}t} \right) \quad (5)$$

126 This equation combined with Eq. (3), yields the following:

$$127 \quad Y = \varepsilon_{\text{Sr-90}} A_{\text{Sr-90}}^0 (1 + \alpha X) \quad (6)$$

128 where  $\alpha = \frac{\varepsilon_{\text{Y-90}}}{\varepsilon_{\text{Sr-90}}}$  and  $X = 1 - e^{-\lambda_{\text{Y-90}}t_d} \left( \frac{1 - e^{-\lambda_{\text{Y-90}}t_d}}{\lambda_{\text{Y-90}}t_d} \right)$ , and  $X$  is the  $^{90}\text{Y}$  saturation ratio corrected

129 for growth during the measurement time (corrected equilibrium fraction). We conducted a regression  
 130 analysis to determine the initial radioactivity of  $^{90}\text{Sr}$ . Eq. (6) is transformed by taking the log of both sides  
 131 to yield the following equation:

$$132 \quad \log Y = \log \left( \varepsilon_{\text{Sr-90}} A_{\text{Sr-90}}^0 \right) + \log (1 + \alpha X) \quad (7)$$

133 This equation is adapted to a non-linear least squares (LSQ) equation to calculate the value of  $\alpha$   
 134 and  $\log \left( \varepsilon_{\text{Sr-90}} A_{\text{Sr-90}}^0 \right)$ . We use only the value of  $\alpha$  to evaluate the absolute values of both  
 135 measurement coefficients in the next step, because the value of  $A_{\text{Sr-90}}^0$  is not equal to the initial solution  
 136 and becomes unknown through the yttrium elimination process where some of  $^{90}\text{Sr}$  is discarded with  $^{90}\text{Y}$ .  
 137 The net CPM of the initial  $^{90}\text{Sr}$  solution in equilibrium shows that Eq. (3) can be converted to the  
 138 following:

$$139 \quad Y = \varepsilon_{\text{Y-90}} A_{\text{Sr-90}}^0 + \varepsilon_{\text{Sr-90}} A_{\text{Sr-90}}^0 = \varepsilon_{\text{Sr-90}} (1 + \alpha) A_{\text{Sr-90}}^0 \quad (8)$$

140 and the resulting equation provides the measurement coefficients for  $^{90}\text{Y}$  and  $^{90}\text{Sr}$ .

141 The evaluation of  $^{90}\text{Sr}$  concentration in the environmental samples would require the consideration  
 142 of coexistence of other radionuclides, even though a careful purification of strontium is conducted. In this  
 143 case Eq. (1) is expressed as:

$$144 \quad Y = \left( \varepsilon_{\text{Y-90}} A_{\text{Sr-90}}^0 \right) X + B \quad (9)$$

145 where  $B = \sum \varepsilon_i A_i$  with  $i = ^{90}\text{Sr}, ^{134}\text{Cs}, ^{137}\text{Cs}, ^{40}\text{K}$ , etc., and  $B$  is regarded as a constant value. After  
 146 the purification of strontium, the increase in net CPM with the corrected equilibrium fraction is applied to

147 regression analysis to yield the value of  $\varepsilon_{Y-90} A_{Sr-90}^0$  as the slope. Then, the value of  $A_{Sr-90}^0$ , the  
148 concentration of  $^{90}\text{Sr}$  in the purified solution, can be determined.

149

## 150 **Results and Discussion**

151 In this study, we used Cherenkov radiation generated by beta particles to detect radionuclides in  
152 vegetation collected around the Fukushima Daiichi Nuclear Power Plant. Table 1 lists the characteristics  
153 of major beta-emitting nuclides released from the power plant as well as those of  $^{40}\text{K}$ , a naturally  
154 occurring radionuclide with a long half-life [28]. The Cherenkov spectra of selected representative  
155 radionuclides are shown in Figure 1. The width of each spectrum peak increases with increased beta  
156 energy, and the spectra obtained for  $^{90}\text{Sr}$  and  $^{134}\text{Cs}$  were derived from similar beta energy profiles. Thus, it  
157 is reasonable to suggest that the spectra of  $^{137}\text{Cs}$  and  $^{89}\text{Sr}$  resemble those of  $^{90}\text{Sr}$  and  $^{40}\text{K}$ , respectively. In  
158 addition, the Cherenkov spectra obtained in this study support the purity of focal radionuclides as well as  
159 the need for further purification of samples.

160 When the same amount of radioactivity is spiked to two measurement samples, the increase in  
161 counting rate is expected to be the same for each unless the effect of quenching in measurement occurs.  
162 We have investigated the contribution of quenching by the addition of  $^{90}\text{Y}$  solution of 0.2 mL in 0.1 M  
163  $\text{HNO}_3$  to the each original measurement sample where  $^{90}\text{Y}$  was in radioactive equilibrium and in 10 mL of  
164 approximately 2 M  $\text{HNO}_3$ . While this treatment changed the total volume and the resulting acid  
165 concentration of the measurement samples, these changes produced no effect to the net CPM, as shown in  
166 the following results. Figure 2 shows the effect of sample solution volume on net CPM where the value of  
167 the net CPM is normalized to the result for the volume of 10 mL, and exhibits good agreement between  
168 sample solutions of volume 5–18 mL. Figure 3 shows the effect of sample acid concentration on net CPM,  
169 where the value of the net CPM is normalized to the result for the concentration of 2 M  $\text{HNO}_3$ , and  
170 exhibits good agreement between  $\text{HNO}_3$  concentrations ranging from 0.3 M to 5.4 M. These results  
171 suggest that the net CPM of  $^{90}\text{Sr}$  of 10 mL in 2 M  $\text{HNO}_3$  will not change by addition of water or nitric  
172 acid at most a few mL, which validates the spike method used to correct for quenching. Figure 4 shows  
173 that the increase in the net CPM of four environmental samples spiked with  $^{90}\text{Y}$  is normalized to the  
174 standard  $^{90}\text{Sr}$  solution spiked. The normalized value of all environmental samples is consistent among all  
175 samples, which means that the measurement coefficient of the resulting solution of  $^{90}\text{Sr}$  extracted and  
176 purified from environmental samples was equal to that of standard  $^{90}\text{Sr}$  solution. The purification of  
177 strontium adequately removed impurities and quenching from the environmental samples and therefore  
178 the radioactivity in the samples can be evaluated without the need for quench correction.

179 Figure 5 shows that the spectrum peak area for  $^{90}\text{Sr}$  changed with the increase of  $^{90}\text{Y}$  in samples  
180 through time. Although the total radioactivity of the sample increased to twice the initial value at full  $^{90}\text{Y}$   
181 saturation, the peak area was much larger than twice the initial value at full  $^{90}\text{Y}$  saturation. This result  
182 suggests the presence of different measurement coefficients between  $^{90}\text{Sr}$  and  $^{90}\text{Y}$ . Table 2 lists the net  
183 CPM of the  $^{90}\text{Sr}$  solution after purification to eliminate  $^{90}\text{Y}$ . The increasing values of the net CPM with  
184 increasing corrected equilibrium fraction yielded the  $\alpha$  value of 16.7, which can be viewed in Figure 6.  
185 The net CPM of 5.83 Bq  $^{90}\text{Sr}$  in equilibrium with  $^{90}\text{Y}$  was  $208 \pm 2$ . The values of  $\alpha$ , net CPM, and

186 radioactivity of  $^{90}\text{Sr}$  were substituted into Eq. (8) to yield measurement coefficients of  $^{90}\text{Sr}$  and  $^{90}\text{Y}$  of  
187  $2.01 \pm 0.02$  and  $33.6 \pm 0.3$  (net CPM/Bq), respectively. These values provided the radioactivity of  $^{90}\text{Sr}$  in  
188 the environmental samples.

189 Radioactivity of  $^{90}\text{Sr}$  in the environmental samples was evaluated from aging of  $^{90}\text{Y}$  using Eq. (9).  
190 The increase in net CPM of  $^{90}\text{Y}$  is listed in Table 3, where the detection limit of net CPM is 5, which was  
191 evaluated with Curie's equation [29], and correspondingly 0.14 Bq from the measurement coefficient.  
192 Although both leaf samples show negligible radioactivity, both bark samples show the increase in net  
193 CPM with aging time. The increase in net CPM with aging provided the radioactivity of  $^{90}\text{Sr}$ , which was  
194 analyzed by the regression analysis and can be viewed in Figure 7. Table 4 lists the resulting specific  
195 radioactivity of  $^{90}\text{Sr}$  and  $^{137}\text{Cs}$ .

196 The radioactivity ratio of  $^{90}\text{Sr}$  to  $^{137}\text{Cs}$  changing with time after the accident provides the migration  
197 tendency of both radionuclides in the environment. The radioactivity levels for all leaf samples collected  
198 from plants 3 km north of the power plant were below the detection limit. The radioactivity levels for  
199  $^{137}\text{Cs}$  in all samples were significant, with particularly high levels in bark samples (up to 173 Bq/g dry  
200 weight). The radioactivity ratios for the bark samples were  $4.2 \times 10^{-3}$  (north) and  $1.2 \times 10^{-2}$  (south),  
201 indicating that the fraction of  $^{90}\text{Sr}$  to total radioactivity levels was one hundredth or less. Table 5  
202 compares radioactivity levels of  $^{90}\text{Sr}$  and  $^{137}\text{Cs}$  in soil collected near the power plant before and after the  
203 nuclear accident from a previously published report [23]. The different release rates of  $^{90}\text{Sr}$  and  $^{137}\text{Cs}$  from  
204 the nuclear reactors caused the radioactivity of  $^{137}\text{Cs}$  to increase to more than one hundred times to the  
205 pre-accident level while the radioactivity of  $^{90}\text{Sr}$  increased to only several times the pre-accident level,  
206 and accordingly the radioactivity ratios decreased from 0.17 to  $8.1 \times 10^{-4}$  and  $4.8 \times 10^{-3}$ . The radioactivity  
207 of bark and soil samples collected in the vicinity of the nuclear power plants showed a larger degree of  
208 contamination in the south area and a larger isotropic release of  $^{90}\text{Sr}$  compared to  $^{137}\text{Cs}$  because between  
209 the north and south area there was difference in one order in radioactivity of  $^{137}\text{Cs}$  while the order of  
210 radioactivity  $^{90}\text{Sr}$  was the same between the north and south area. The radioactivity ratios of  $^{90}\text{Sr}$  to  $^{137}\text{Cs}$   
211 in the bark samples were at least 2.4 times those of the soil samples. The radioactivity ratio in soil and  
212 bark samples would be the same value immediately after the accident due to the same contamination  
213 history at each location where the samples were collected. However, the radioactivity ratio of soil and  
214 bark samples, collected 4 months and 26 months after the accident, respectively, were different from each  
215 other, showing the different migration rate of  $^{90}\text{Sr}$  and  $^{137}\text{Cs}$ . The increase in the radioactivity ratio in bark  
216 samples can be ascribed to the accumulation of  $^{90}\text{Sr}$  to bark or the diffusion of  $^{137}\text{Cs}$  from bark. The  
217 accumulation of  $^{90}\text{Sr}$  through root uptake is negligible because the migration rate of  $^{90}\text{Sr}$  in soil is reported  
218 to be 0.2 – 1.0 cm/yr [30-32]. The rapid translocation of  $^{137}\text{Cs}$  from bark into the wood was observed in  
219 Fukushima forest [33]. This increase in the radioactivity ratio in bark samples with time shows slower  
220 migration of  $^{90}\text{Sr}$  than  $^{137}\text{Cs}$  in bark and tree. The effect of different migration would be expected to cause  
221 considerable variation in radioactivity ratio from the initial value. The determination of  $^{90}\text{Sr}$  in  
222 environmental samples is required to avoid suffering from unexpected  $^{90}\text{Sr}$  hot spots.'

223

224

225 **Conclusions**

226 We measured the specific activity of  $^{90}\text{Sr}$  and  $^{137}\text{Cs}$  in leaf and bark samples collected in the vicinity  
227 of the Fukushima Daiichi Nuclear Power Plants in May 2013. The radioactivity of  $^{90}\text{Sr}$  was quantitatively  
228 measured by using Cherenkov counting, where purified  $^{90}\text{Sr}$  and  $^{90}\text{Y}$  from the standard solution of  $^{90}\text{Sr}$   
229 were used to evaluate the measurement coefficient of Cherenkov counting and to verify the determination  
230 without any quench correction. The radioactivity of both radionuclides in the bark samples was larger  
231 than that in the leaf samples. The slower migration rate of  $^{90}\text{Sr}$  compared to  $^{137}\text{Cs}$  was shown by  
232 comparison to the radioactivity ratios of both radionuclides in soil samples collected in July 2011. The  
233 rough tendency of the migration in trees is shown; however, further analysis is required for the discussion  
234 of the migration of  $^{90}\text{Sr}$  in the environment.

235

### 236 **Acknowledgments**

237 We wish to thank Mr. Mitsuyuki KONNO and Mr. Satoru MATSUZAKI for their help in collecting  
238 environmental samples. This work was supported by the KUR Research Program for Scientific Basis of  
239 Nuclear Safety.

240

### 241 **References**

242 [1] Itthipoonthanakorn T, Krisanangkura P, Udomsomporn S (2013) J Radioanal Nucl Chem 297:  
243 419-421

244 [2] Povinec PP, Sykora I, Gera M, Holy K, Brest'akova L, Kovacik A (2013) J Radioanal Nucl Chem 295:  
245 1171-1176

246 [3] Lee SH, Heo DH, Kang HB, Oh PJ, Lee JM, Park TS, Lee KB, Oh JS, Suh JK (2013) J Radioanal  
247 Nucl Chem 296: 727-731

248 [4] Tumey SJ, Guilderson TP, Brown TA, Broek T, Buesseler KO (2013) J Radioanal Nucl Chem 296:  
249 957-962

250 [5] Nakanishi TM, Kobayashi NI, Tanoi K (2013) J Radioanal Nucl Chem 296: 985-989

251 [6] Furuta E (2013) J Radioanal Nucl Chem 297: 337-342

252 [7] Maxwell SL, Culligan BK, Shaw PJ (2013) J Radioanal Nucl Chem 295: 965-971

253 [8] Mahmood ZUW, Ariffin NAN, Ishak AK, Mohamed N, Yii MW, Ishak K, Pa'wan Z (2012) J  
254 Radioanal Nucl Chem 291: 901-906

255 [9] Dai X, Kramer-Tremblay S (2011) J Radioanal Nucl Chem 289: 461-466

256 [10] Lopes I, Madruga MJ, Mourato A, Abrantes J, Reis M (2010) J Radioanal Nucl Chem 286: 335-340

257 [11] Maxwell SL, Culligan BK, Shaw PJ (2010) J Radioanal Nucl Chem 286: 273-282

258 [12] Karacan F (2011) J Radioanal Nucl Chem 288: 685-691

259 [13] Grahek Z, Nodilo M (2012) J Radioanal Nucl Chem 293: 815-827

260 [14] Grahek Z, Karanovi G, Nodilo M (2012) J Radioanal Nucl Chem 292: 555-569

261 [15] Maxwell SL, Culligan BK (2009) J Radioanal Nucl Chem 279: 105-111

262 [16] Maxwell SL, Culligan BK (2009) J Radioanal Nucl Chem 279: 901-907

263 [17] Lee MH, Park TH, Park JH, Song K, Lee MS (2013) J Radioanal Nucl Chem 295: 1419-1422

264 [18] Solecki J, Kruk M (2011) J Radioanal Nucl Chem 289: 185-190

265 [19] Bhade SPD, Reddy PJ, Narayanan A, Narayan KK, Babu DAR, Sharma DN (2010) J Radioanal



266 Nucl Chem 284: 367-375  
267 [20] Solecki J, Kruk M, Orzel J (2010) J Radioanal Nucl Chem 286: 27-32  
268 [21] Dai X, Cui Y, Kramer-Tremblay S (2013) J Radioanal Nucl Chem 296: 363-368  
269 [22] Popov L, Mihailova G, Naidenov I (2010) J Radioanal Nucl Chem 285: 223-237  
270 [23] Fukushima prefectural government (2012)  
271 <http://wwwcms.pref.fukushima.jp/download/1/dojou120406.pdf> (in Japanese)  
272 [24] Shibahara Y, Kubota T, Fukutani S, Fujii T, Yoshikawa M, Shibata T, Ohta T, Takamiya K, Okumura  
273 R, Mizuno S, Yamana H (submitted) J Radioanal Nucl Chem  
274 [25] Sato J, Sato K (1977) Geochemical Journal 11: 261 - 266  
275 [26] Sato J, Hirose T, Sato K (1980) Int J App Rad Iso 31: 130-132  
276 [27] Kubota T, Fukutani S, Ohta T, Mahara Y (2013) J Radioanal Nucl Chem 296:981-984  
277 [28] Firestone RB, Shirley VS, Baglin CM, Chu SYF, Zipkin J (1996) The 8th edition of the Table of  
278 Isotopes, book and CD-ROM, John Wiley & Sons, Inc.  
279 [29] Currie LA (1968) Anal Chem 40: 586-593  
280 [30] Herranz M, Romero L.M, Idoeta R, Olondo C, Valino F, Legarda F (2011) J Environmental  
281 Radioactivity 102: 987-994  
282 [31] Mahara Y (1993) J Env Qual 22: 722-730  
283 [32] Fernandez J.M, Piauult E, Macouillard D, Juncos C (2006) J Environmental Radioactivity 87:  
284 209-226  
285 [33] Kuroda K, Kagawa A, Tonosaki M (2013) J Environmental Radioactivity 122: 37-42  
286  
287  
288  
289

290 **Tables and Figures**

291 Table 1 Maximum energy and emission ratio of major beta-emitting radionuclides in environmental  
292 samples

293

294 Table 2 Increase in net counting rate of purified  $^{90}\text{Sr}$  solution with the corrected equilibrium fraction of  
295  $^{90}\text{Y}$  (i.e., growth of  $^{90}\text{Y}$ )

296

297 Table 3 Increase in net counting rate of purified  $^{90}\text{Sr}$  recovered from vegetation samples with the  
298 corrected equilibrium fraction of  $^{90}\text{Y}$

299

300 Table 4 Radioactivity levels of  $^{90}\text{Sr}$  and  $^{137}\text{Cs}$  found in vegetation samples collected near the Fukushima  
301 Daiichi Nuclear Power Plant

302

303 Table 5 Radioactivity levels of  $^{90}\text{Sr}$  and  $^{137}\text{Cs}$  found in soil samples collected near the Fukushima Daiichi  
304 Nuclear Power Plant, as reported by [23]

305

306 Figure 1 Comparison of Cherenkov radiation spectra for  $^{90}\text{Y}$ ,  $^{40}\text{K}$ ,  $^{137}\text{Cs}$ , and  $^{90}\text{Sr}$

307

308 Figure 2 Effect of sample solution volume with the same amount of  $^{90}\text{Sr}$  on Cherenkov counting rates,  
309 normalized to the rate at 10 mL volume

310 SD:  $2\sigma$

311

312 Figure 3 Effect of acid concentration on Cherenkov counting rates, normalized to the rate at the  
313 concentration of 2 M  $\text{HNO}_3$

314 SD:  $2\sigma$

315

316 Figure 4 Increase ratio in net counting rate in  $^{90}\text{Sr}$  from vegetation samples by the spike of purified  $^{90}\text{Y}$  in  
317 comparison to the standard  $^{90}\text{Sr}$  solution spiked for the same amount of  $^{90}\text{Y}$ .

318 SD:  $2\sigma$

319

320 Figure 5 Change in Cherenkov spectra for purified  $^{90}\text{Sr}$  solution with respect to the corrected equilibrium  
321 fraction of  $^{90}\text{Y}$ .

322

323 Figure 6 Fitting line defined in Eq. (7) to evaluate the ratio of the detection coefficient of  $^{90}\text{Y}$  and  $^{90}\text{Sr}$ ,  $\alpha$ ,  
324 using the values in Table 2

325

326 Figure 7 Regression analysis for the evaluation of radioactivity of  $^{90}\text{Sr}$  in vegetation samples (closed  
327 circle: #1 bark *Metasequoia*; open circle: #2 bark *Cryptomeria japonica*)

328

329 Table 1

330

Nuclide	Maximum $E_{\beta}$ (MeV)	Emission ratio
$^{40}\text{K}$	1.311	
$^{89}\text{Sr}$	1.495	
$^{90}\text{Sr}$	0.546	
$^{90}\text{Y}$	2.280	
$^{134}\text{Cs}$	0.658	70.2%
	0.415	2.5%
	0.089	27.3%
$^{137}\text{Cs}$	1.176	5.6%
	0.514	94.4%

331

332

333 Table 2

334

Aging Time (hr)	Counting Time (hr)	X*	Net CPM
0.4	0.5	0.007	28.5 ± 1.5
44.4	0.5	0.383	174.0 ± 2.6
81.7	0.5	0.588	260.8 ± 3.2
123.6	0.5	0.738	323.2 ± 3.5
621.4	0.5	0.999	438.2 ± 4.0

335 \*X: Corrected Equilibrium Fraction

336

337

#1 Bark *Metasequoia*

Aging Time (hr)	$X^*$	Net CPM
112.0	0.71	23.38 ± 0.98
146.7	0.80	25.00 ± 0.99
216.5	0.91	28.12 ± 1.02
289.1	0.96	29.59 ± 1.03
327.9	0.97	30.17 ± 1.03
371.4	0.98	30.08 ± 1.03

$$A = 25.91 \pm 1.24$$

$$B = 4.73 \pm 1.11$$

#2 Bark *Cryptomeria japonica*

Aging Time (hr)	$X^*$	Net CPM
131.8	0.76	6.34 ± 0.82
170.6	0.85	7.41 ± 0.83
214.1	0.90	8.34 ± 0.83
307.5	0.96	8.43 ± 0.84

$$A = 11.08 \pm 2.13$$

$$B = -2.00 \pm 1.85$$

#3 Leaf *Cryptomeria japonica*

Aging Time (hr)	$X^*$	Net CPM
136.0	0.78	1.81 ± 0.77
174.8	0.85	1.92 ± 0.77
218.3	0.91	2.02 ± 0.77
311.7	0.97	2.15 ± 0.77

#4 Leaf *Artemisia*

Aging Time (hr)	$X^*$	Net CPM
49.8	0.43	1.51 ± 0.76
103.8	0.68	1.46 ± 0.75
147.5	0.80	0.88 ± 0.76

340  $X^*$ : Corrected equilibrium fraction

341 Detection limit: net CPM = 5

342

343

344 Table 4

345

Sample	Location*	<sup>90</sup> Sr (Bq/g)	<sup>137</sup> Cs (Bq/g)	<sup>90</sup> Sr / <sup>137</sup> Cs
#1 Bark <i>Metasequoia</i>	2 km south	0.73 ± 0.04	172.9 ± 2.0	(4.2 ± 0.2) × 10 <sup>-3</sup>
#2 Bark <i>Cryptomeria japonica</i>	3 km north	0.31 ± 0.06	26.9 ± 0.5	(1.2 ± 0.2) × 10 <sup>-2</sup>
#3 Leaf <i>Cryptomeria japonica</i>	3 km north	< DL**	10.4 ± 0.2	
#4 Leaf <i>Artemisia</i>	3 km north	< DL**	4.9 ± 0.2	

346 \* Location: Distance from the Fukushima Daiichi Nuclear Power Plant Unit No. 1

347 \*\* DL: 0.11 Bq/g

348

349

350 Table 5

351

Location\*: 2 km south

Sampling Year	2005	July 2011
<sup>90</sup> Sr (Bq/g)	ND**	0.0808
<sup>137</sup> Cs (Bq/g)	ND**	99.7
<sup>90</sup> Sr/ <sup>137</sup> Cs		$8.1 \times 10^{-4}$

352

Location\*: 3 km north

Sampling Year	2005	July 2011
<sup>90</sup> Sr (Bq/g)	0.0030	0.0149
<sup>137</sup> Cs (Bq/g)	0.0173	3.08
<sup>90</sup> Sr/ <sup>137</sup> Cs	0.17	$4.8 \times 10^{-3}$

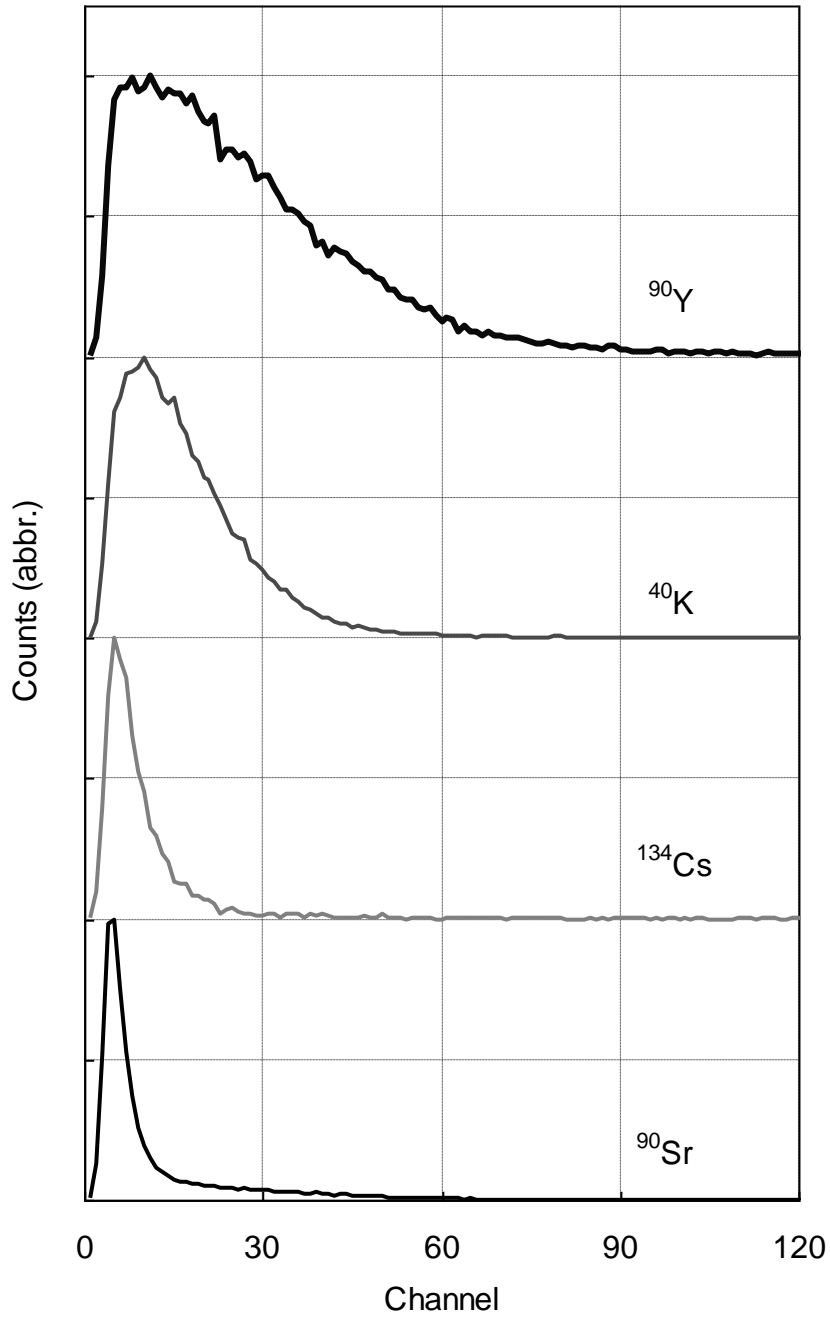
353 Location\*: Distance from the Fukushima Daiichi Nuclear Power Plant Unit No. 1

354 ND\*\*\*: Not detected

355

356

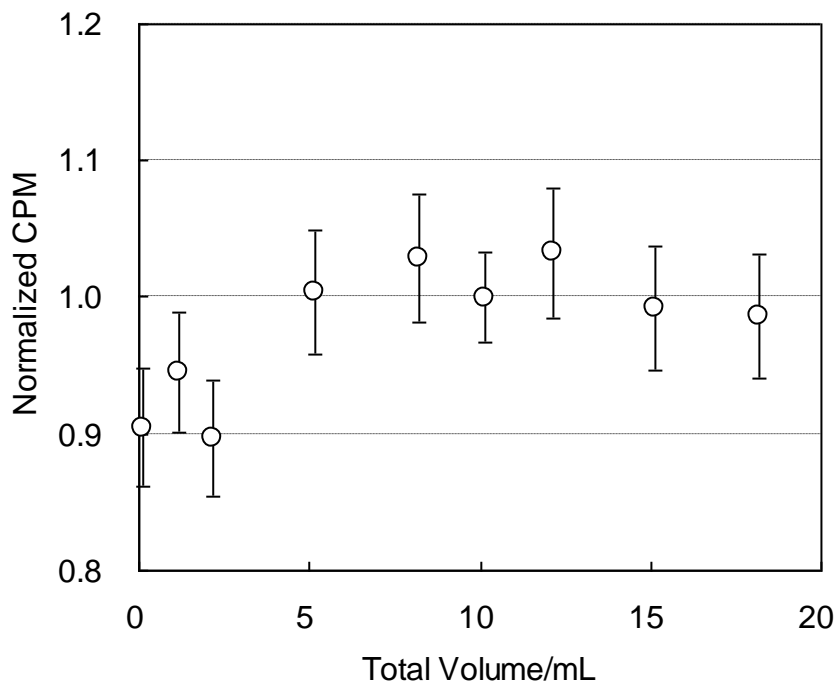
357 Figure 1  
358  
359  
360



361  
362



363 Figure 2

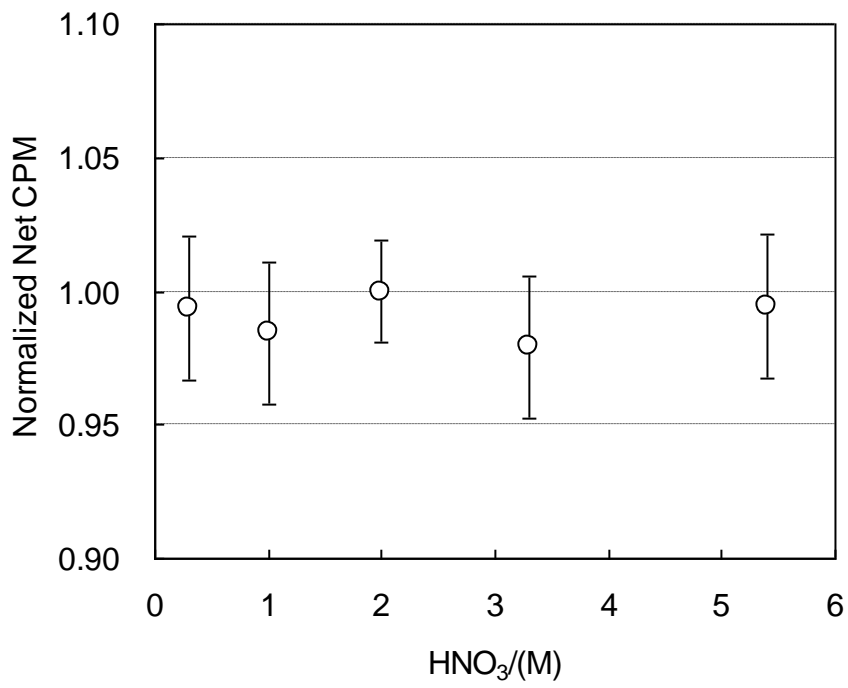


364

365

366

367 Figure 3



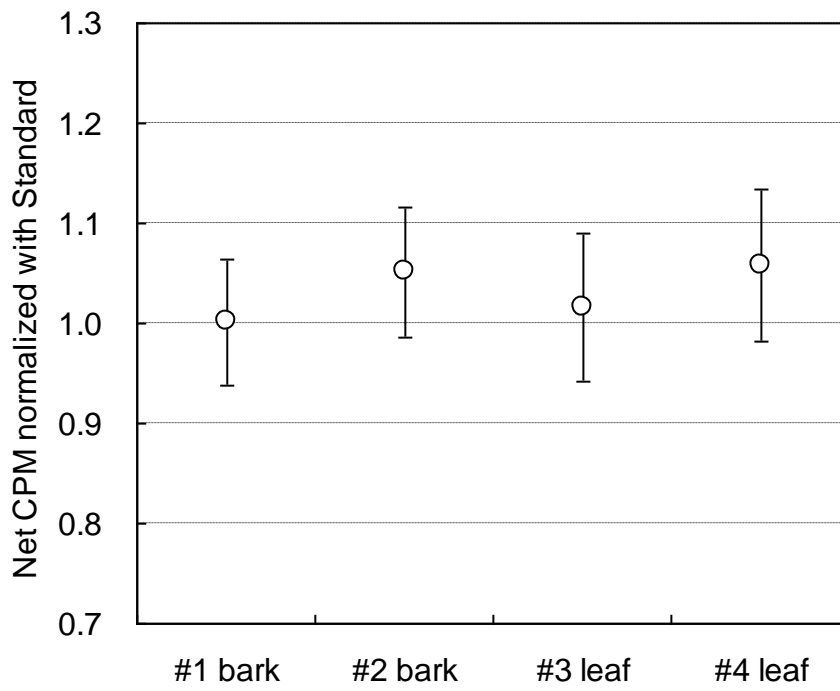
368

369

370

371 Figure 4

372

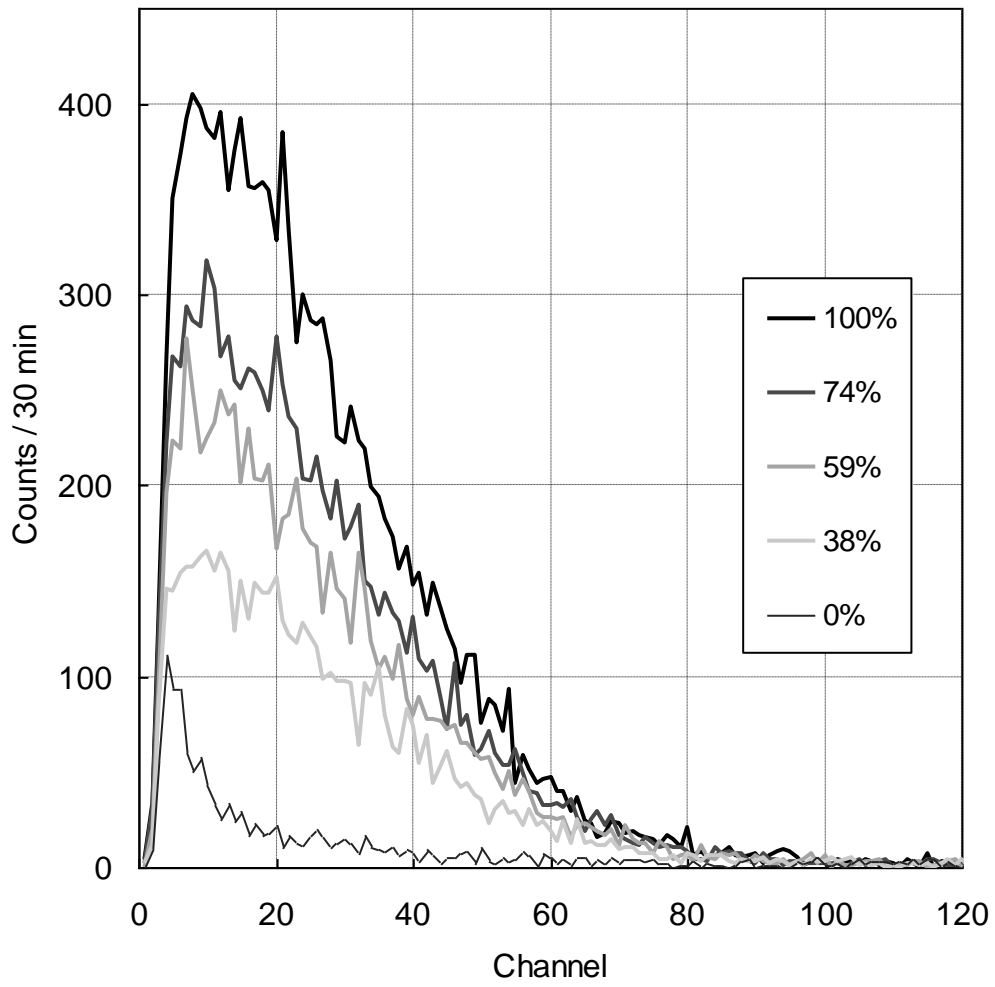


373

374

375 Figure 5

376



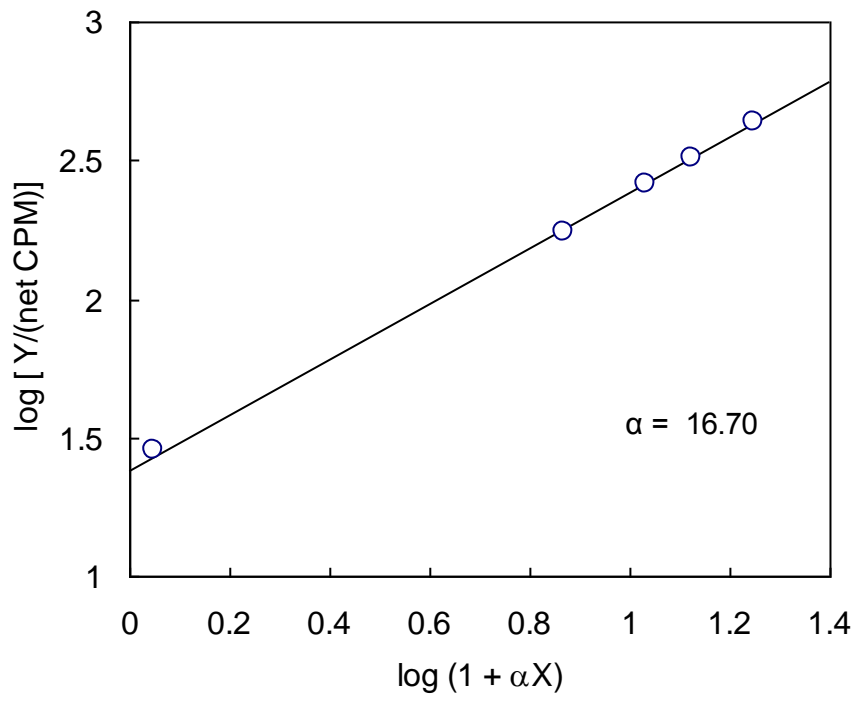
377

378

379

380 Figure 6

381

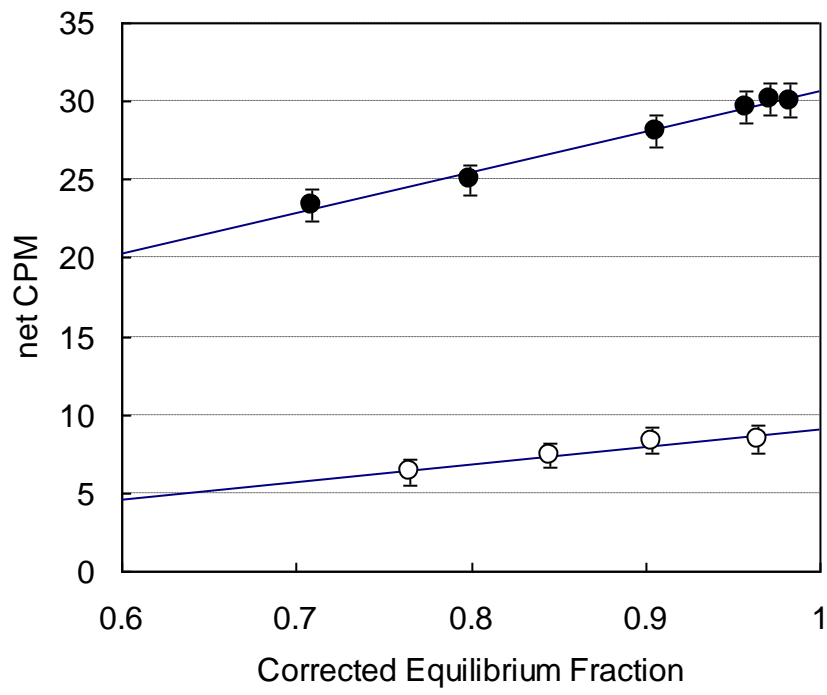


382

383

384 Figure 7

385



386

387